Noble Metal Substrate Identity Effects on the Self-Assembly, Dynamics, and Dehydrocyclization Reaction of Octaethylporphyrin Molecules

*Jeremy F. Schultz, Nan Jiang**

Department of Chemistry, University of Illinois at Chicago, Chicago, Illinois 60607, United States

ABSTRACT

Conjugated organic molecules are attractive candidates to realize platforms on surfaces, where self-assembly and molecule–substrate interactions can be used to impart tailored characteristics at the interface or enable single-molecule studies of chemistry. Scanning tunneling microscopy (STM) enables the interrogation of these surfaces at the atomic-scale, providing a method to image and develop understandings of fundamental interactions. This includes the ability to identify individual products of any chemical reactions that may be an end result of sufficiently strong molecule–substrate interactions. Here, ultrahigh vacuum STM was used to study the self-assembly and surface-catalyzed reactions of octaethylporphyrin on noble metal substrates: Cu(100), Ag(100), Au(100), and Ag(110). The substrate identity and facet were found to substantially determine the nature of molecule–substrate interactions. As a result, the temperature necessary to drive the dehydrocyclization of peripheral ethyl groups, resulting in the formation of

tetrabenzoporphyrin molecules, was found to differ significantly between substrates. STM provided the ability to probe and manipulate molecules on the surface, revealing single-molecule behavior and therefore a fundamental view of molecule–substrate interactions and a surface-catalyzed reaction.

INTRODUCTION

The ability to develop useful functionalities of organic thin films requires the fine control of minute factors that govern self-assembly,[1] which includes molecule–substrate and intermolecular interactions[2] as well as any on-surface reactions that can either contribute to bottom-up assembly methods or interrupt fabrication processes.[3-6] Molecular selection is a powerful means to direct the on-surface formation of nanoarchitectures through principles of rational design,[7-10] while the substrate choice can be used to guide and steer the process,[11-12] potentially providing templating effects. Taken all together, the self-assembly of molecules on a surface represents a balance between molecule–substrate and molecule–molecule interactions.[13-14] Although self-assembly relies on the behavior of a molecular ensemble, a close examination of individual molecules can provide a picture of the fundamental forces that underlie bottom-up fabrication methods and on-surface chemistry.

In this regard, scanning tunneling microscopy (STM) is an ideal method to study the behavior and reactions of organic molecules on metal surfaces, due to its ability to image surfaces at the atomic level[15] and even perform molecular and atomic manipulations.[16] STM has found extensive applications in the study of functional organic thin films, as well as in the study of chemical reactions on surfaces.[17-21] Surface assemblies of porphyrins specifically are of special interest due to their rich electronic and photonic properties,[22] where porphyrin derivatives have

important roles in biological processes as well as hybrid molecular and photovoltaic devices.[23] Generally, porphyrins are remarkably stable, ultrahigh vacuum (UHV) studies rely on thermal sublimation onto metal substrates in order to prepare thin films.[22, 24-25] However, it is possible for porphyrins to undergo surface catalyzed reactions.[26] These processes can include self-metalation of the porphyrin core,[27-31] as well as intramolecular and intermolecular reactions of peripheral functional groups.[22, 32-34] Importantly, investigations of the chemistry of functional groups provide the ability to perform single-molecule studies of on-surface reactions that may otherwise be inaccessible with STM. Well-defined single crystal surfaces of copper, gold, and silver, typical in UHV-STM studies, are generally considered inert for dehydrocyclization reactions, since alkanes and other small hydrocarbons can desorb from these surfaces below the temperatures necessary to catalyze dehydrogenation reactions.[34] In contrast, the inclusion of alkyl groups on the periphery of a porphyrin macrocycle offers a stable molecular platform to consider an intramolecular reaction with single-molecule resolution. Molecule–substrate interactions that occur between the aromatic macrocycle and surface atoms can anchor the molecule, while the peripheral functional groups can undergo a chemical reaction. Importantly, metalation of the porphyrin core can substantially affect the interactions of the conjugated macrocycle with the substrate.[35-36] The chemical reactions of peripheral functional groups can either result in new covalent networks or destabilize the intermolecular interactions that stabilized the original nanostructure. Therefore, it becomes necessary to consider both self-assembly and chemical reactions with single-molecule sensitivity, achievable with STM.[37]

Here we have applied UHV low temperature STM to the study of octaethylporphyrin (OEP) on a variety of noble metal substrates: Cu(100), Ag(100), Au(100), and Ag(110). OEP is a synthetic porphyrin that consists of a porphyrin macrocycle that is essentially planar, with ethyl

groups substituted at the eight pyrrolic or β positions (Figure 1a).[38] OEP was chosen due to the presence of these peripheral alkyl groups that can mediate intermolecular interactions as well as undergo thermally induced reactions. Specifically, OEP provides a molecular platform to consider the surface-catalyzed reactions of short alkyl chains. Interactions of the porphyrin macrocycle with the substrate stabilize the larger molecule on the surface and enable STM imaging of individual molecules and their orientation relative to the substrate. Ultimately, the characterization of single-molecule behavior provides unique insight into these systems and on-surface reactions.

EXPERIMENTAL METHODS

Experiments took place in a variable temperature UHV scanning tunneling microscope system (Unisoku Co., Ltd.) at a base pressure of 5.0×10^{-11} Torr previously described in more detail elsewhere.[39] The metal single crystals, Cu(100), Ag(100), Au(100), and Ag(110), were prepared in a preparation chamber with a base pressure of 1.0×10^{-10} Torr and then transferred through a gate valve into the STM chamber for observation. The substrates were cleaned by standard cycles of argon ion sputtering followed by thermal annealing. The octaethylporphyrin (OEP) molecules were purchased from Frontier Scientific and deposited via a K-cell molecular evaporator (200 ℃) to obtain submonolayer coverage. The substrates were at room temperature during deposition. The thermal annealing of OEP molecules on substrates was carried out by indirect heating through a tungsten filament located behind the sample. The process used to determine the annealing temperatures used for each substrate is described in the Supporting Information. All STM images were acquired at liquid nitrogen temperature (~78 K). Electrochemically etched Ag[40] and Pt/Ir tips were used for STM imaging. Gwyddion was used for STM image processing.[41]

RESULTS AND DISCUSSION

The self-assembly and substrate-induced reactions of OEP were investigated on a variety of noble metal surfaces. Specifically, Cu(100), Ag(100), Au(100), and Ag(110) surfaces were considered in order to assess the effects of substrate identity on molecular behavior and reactivity towards the catalysis of a dehydrocyclization reaction. Experiments began with the Cu(100) surface, which was expected to serve as the most reactive surface as a benchmark to compare the other surfaces against.[42-43]

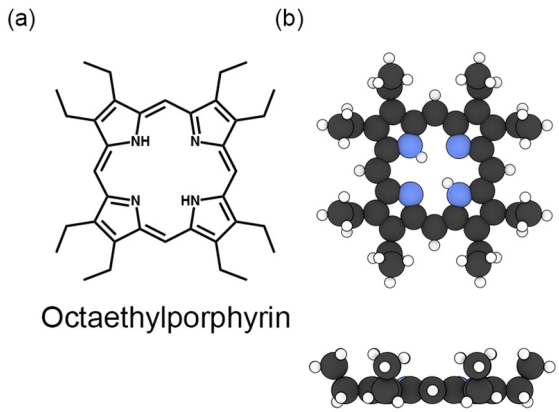

Figure 1. (a) Chemical structure of an octaethylporphyrin (OEP) molecule. (b) 3D model of OEP in top and side view.

In the case of large molecules, the molecule–substrate interactions can have significant effects on the binding conformation, as flexibility in the molecular structure can result in conformations that differ significantly from gas phase and crystal structures.[44-45] Previous studies of octaethylporphyrin derivatives have established that these molecules adsorb in a flat, undistorted conformation where the eight ethyl groups point away from the surface via a variety of methods that include: STM,[46-47] photoelectron spectroscopies such as X-ray photoelectron spectroscopy and ultraviolet spectroscopy,[48] high resolution electron energy loss spectroscopy,[34] and near edge X-ray adsorption fine structure.[49] This conformation is shown in Figure 1b. Notably, this allows for

interactions between the iminic and pyrrolic nitrogen atoms of the macrocycle core with the surface metal atoms, which can serve to stabilize the molecule on a surface.[50]

A room temperature deposition of OEP onto the Cu(100) surface was found to result in isolated molecules with no self-assembly or long-range ordering, as can be seen in Figure 2a and also in a large range STM image presented in the Supporting Information, Figure S1. All of the isolated OEP molecules were found to adopt an identical orientation on the surface, suggesting a strong molecule-substrate interaction that may be mediated through the iminic nitrogen atoms of the central porphine macrocycle.[51] At higher coverages, the strong molecule–substrate interactions results Due to the presence of isolated molecules, it was possible to image a single OEP molecule (Figure 2b) and identify its orientation relative to the underlying atomic lattice as illustrated in Figure 2c.

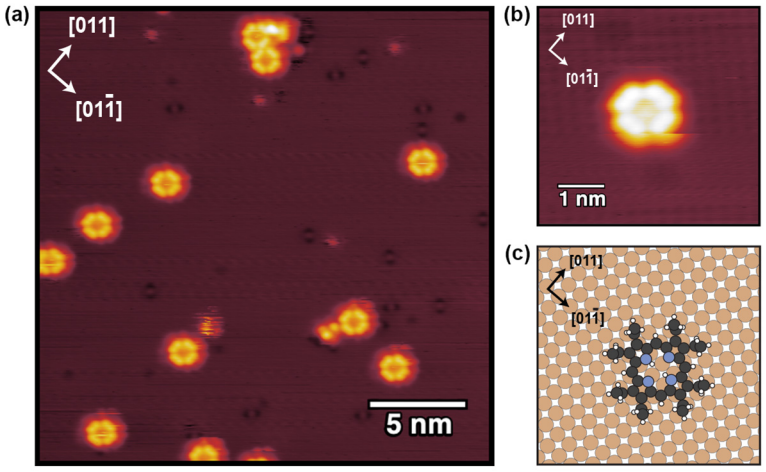

Figure 2. STM images and model of OEP on Cu(100). (a) STM image showing the orientation of OEP molecules relative to the close packed directions of the substrate ($U = -1$ V, $I = 150$ pA). (b) STM image of a single OEP molecule representative of the orientation of all observed molecules on this surface with the atomic lattice of the substrate faintly visible ($U = +1$ V, $I = 100$ pA). (c) Illustration of a molecular model of OEP on the Cu(100) surface with the atomic lattice aligned with the STM images.

In order to observe the formation of any reaction products and their effects on molecule–substrate interactions, the sample was thermally annealed. The result of this process is shown in

Figure 3a. The molecules now take on a new distinct appearance in STM images. The appearance of individual molecules is significantly changed to four-lobe structures with a central cavity that is easily resolved. In previous work, a thermal annealing has been found to result in the dehydrogenation and cyclization of the peripheral ethyl groups of OEP molecules, resulting in the formation of tetrabenzoporphyrin (TBP) molecules, as confirmed with STM imaging and subsequent comparisons with widely available phthalocyanine molecules.[52] Based upon previous studies, the species observed here can be defined as TBP, where the chemical structure is shown in Figure 3b.[46] The suggested reaction mechanism, shown in Figure 3c, involves the dehydrogenation of the peripheral ethyl groups followed by electrocyclic ring closure to form a six-membered carbon ring, which through a subsequent further dehydrogenation step forms the final benzene rings that are fused to the pyrrole subunits. Figure 3d illustrates the planarity of the TBP structure, which arises from the aromaticity throughout the molecule. Here, it was found that a 600 K annealing for 15 minutes was sufficient to induce the transformation of all of the OEP molecules on the copper surface into TBP molecules.

Interestingly, the TBP molecules adopt one of two orientations on the surface relative to the close packed directions of the (100) substrate with equal probability, as highlighted by the color-coded X's overlaid Figure 3a. The orientation of a benzopyrrole subunit is either 30° clockwise or counterclockwise to the $[01\bar{1}]$ direction of the Cu(100) surface, as illustrated with models in Figure 3e. Further, there appears to be the potential for intermolecular homocoupling reactions. STM imaging provides the tentative identification of oligomers composed of multiple TBP molecules due to dehydrogenative homocoupling. A trimer and dimers are apparent in Figure 3a. This process has previously been observed to occur for free-base porphine molecules on a metal surface.[53-54] Overall, the strong interactions of OEP with the Cu(100) substrate were found

to prohibit the self-assembly of larger supramolecular structures, as well as catalyze the dehydrocyclization reaction at 600 K where the potential products may include oligomer formation.

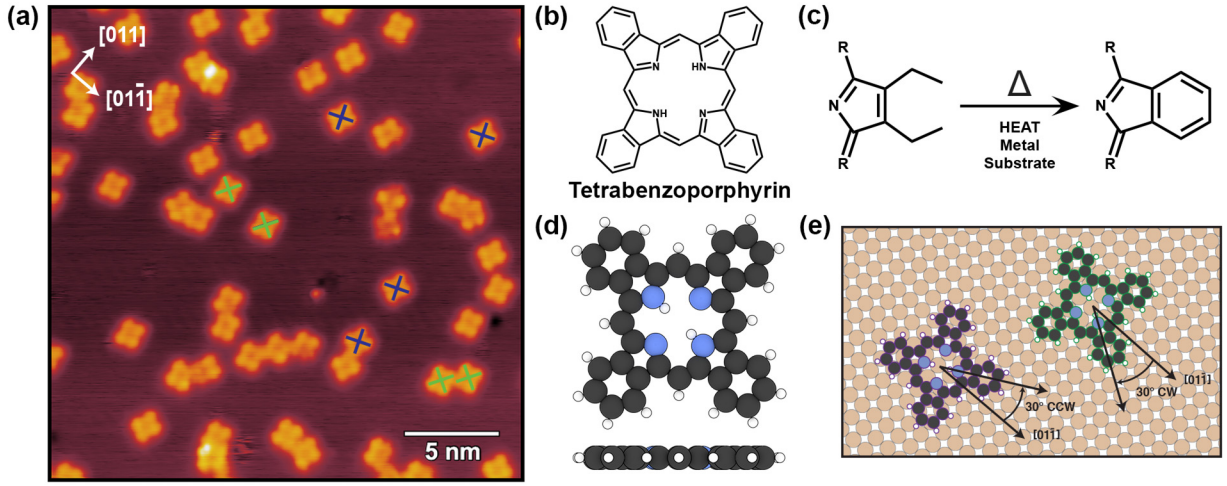

Figure 3. (a) STM image of the products that form following a 600 K thermal annealing for 15 minutes of the OEP on Cu(100) sample. Tetrabenzoporphyrin (TBP) molecules of two possible orientations are apparent with color-coded X's overlaid to highlight them ($U = -1$ V, $I = 150$ pA). (b) Chemical structure of a TBP molecule. (c) Thermally induced metal surface catalyzed reaction of ethyl groups to form a benzopyrrole unit. (d) Space filling model of TBP in top and side view. (e) Illustration of the two observed possible orientations of TBP molecules on Cu(100). The direction of a benzopyrrole subunit is evaluated relative to the $[01\bar{1}]$ direction. The models are color-coded to match the molecules marked with X's in (a).

In order to consider the effects of the substrate on the behavior and reaction of OEP molecules, OEP was next considered on a Ag(100) substrate. Here, the OEP molecules were found to self-assemble into densely packed molecular islands on Ag(100) with no clear instances of isolated individual molecules observed on the surface (Figure 4). STM imaging enables the ability to resolve molecular behavior as well as characterize the order of self-assembled molecular islands. In order to consider the nature of the self-assembly in finer detail, a zoomed-in STM image is presented in Figure 4a. OEP molecules of adjacent rows, that orient along a close packed direction of the Ag(100) substrate, were observed to differ by a slight degree of rotation (~10°) resulting in

a relatively large unit cell as noted in Figure 4a. A close packed structure was observed where peripheral ethyl groups fit together, resulting in dense self-assembled molecular islands where molecules within an island are stabilized on the surface by intermolecular interactions, while molecules on the exterior of self-assemblies are comparatively unstable.[55]

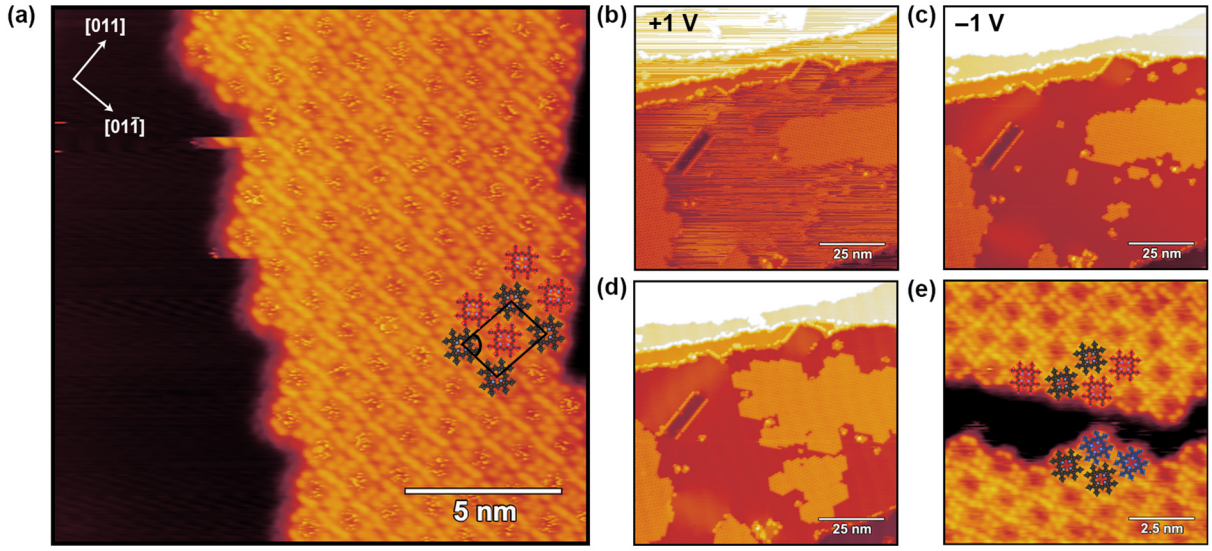

Figure 4. STM images of OEP on Ag(100). (a) High resolution showing self-assembly. Molecular models of the two orientations are color-coded and overlaid. A unit cell is defined that roughly aligns with the close packed directions of the substrate. The dimensions of the unit cell are $1.49\ \text{nm} \times 2.18\ \text{nm}$ where the designated angle is 84° ($U = -1\ \text{V}, I = 150\ \text{pA}$). (b) and (c) STM images showing the effects of applied biases on molecular diffusion, the respective applied biases are noted on the image [(b) $U = +1\ \text{V}, I = 150\ \text{pA}$; (c) $U = -1\ \text{V}, I = 150\ \text{pA}$]. (d) The final self-assemblies observed following a series of consecutive scans with alternating applied biases of a given area shown in (b) and (c) ($U = -1\ \text{V}, I = 150\ \text{pA}$). (e) Zoomed-in STM images of the two adjacent molecular islands with molecular models overlaid, the observed rotations of molecules are highlighted by colored outlines ($U = -1\ \text{V}, I = 150\ \text{pA}$).

While scanning with the STM, the applied bias voltages used for STM imaging were found to strongly affect the acquired images. As shown in Figure 4b, a positive applied voltage resulted in significant scratch-like artifacts that align with the fast scan direction of the STM tip. These artifacts can be attributed to a diffusing species on the surface.[56] The next successive scan acquired over the same area with a negative applied voltage revealed the formation of a few new molecular islands (Figure 4c). A series of STM images were acquired over this area with alternating applied

biases resulting in the growth of a new molecular island, as well as the noticeable growth of pre-existing self-assemblies. The final result of this process appears in Figure 4d. For completeness, the full series of STM images with alternating biases are included in the Supporting Information as Figure S2. These images show the steady growth of molecular islands as molecules diffuse on the surface with a positive applied bias, suggesting that an applied electric field can be used to influence the diffusivity of OEP on the Ag(100) surface. This has been previously observed for iron phthalocyanine on Au(111), suggesting the ability to influence the formation and dissipation of molecular patterning on a surface.[57] Interestingly, the two large adjacent islands shown in Figure 4d never merged into one singular island. A closer examination of the self-assembled molecules that compose these two islands, shown in Figure 4e, reveals that molecules within alternating rows of each island differ by $\sim 25°$ compared between islands, suggesting that this slight difference in rotation prevents these two domains from merging. These molecules have been outlined with red and blue respectively in the molecular models overlaid on the STM image. Overall, STM imaging resulted in the characterization of local self-assemblies as well as the ability to use the applied electric field to influence molecular diffusion and dynamically grow a new domain of OEP molecules.

In comparison to the Cu(100) surface, a thermal annealing of $700\ \mathrm{K}$ sustained for 15 minutes was found to result in the reaction of all OEP molecules on the Ag(100) substrate, as confirmed with STM imaging. As can be seen in Figure 5a, thermal annealing results in the total disruption of molecular self-assembly, as molecules now appear isolated on the surface. Significantly, TBP molecules were observed to again adopt one of two orientations on the surface, where a benzopyrrole unit is either $30°$ clockwise or counterclockwise to the $[01\bar{1}]$ direction of the Ag(100) substrate. These possible species are highlighted with green and purple X's

respectively in Figure 5a, and an illustration showing the orientation of molecular models on the atomic surface appears adjacent in Figure 5b. Through assessing a number of STM images, the two orientations were found to occur in an equal ratio, suggesting degeneracy between these two possibilities on the surface.

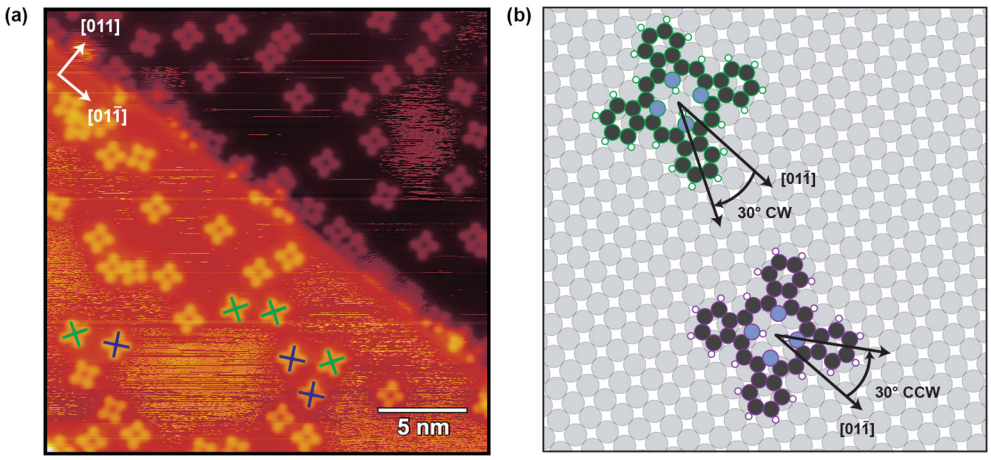

Figure 5. (a) STM image of the products that form following a 700 K thermal annealing for 15 minutes of the OEP on Ag(100) sample. TBP molecules of two possible orientations are apparent with a few color-coded X's overlaid ($U = -0.5$ V, $I = 100$ pA). (b) Illustration of the two observed possible orientations of TBP molecules on Ag(100). The direction of a benzopyrrole subunit is evaluated relative to the $[01\bar{1}]$ direction. The models are color-coded to match the molecules marked with X's in (a).

In order to develop a more complete understanding of the self-assembly and substrate-catalyzed reaction of OEP on coinage metals, OEP was next deposited onto a Au(100) surface using the same previously established parameters. The gold surface was expected to serve as a more inert substrate compared to silver and copper, while the corrugation of the Au(100) reconstruction may offer potential templating effects for self-assembly and chemical reactions. An STM image of OEP on Au(100), Figure 6a, suggests that the reconstruction may interfere with the formation of larger self-assemblies. Rather than the large molecular islands observed on Ag(100), here OEP molecules adopt more one-dimensional self-assemblies, forming relatively stable two- or three-molecule wide features where their growth direction is oriented perpendicular to the

modulation of the surface reconstruction. The relative lack of intermolecular interactions results in self-assemblies that are easily affected by the scanning STM tip. As as result, it was not possible to clearly define the orientation of individual OEP molecules on the Au(100) surface. Through progressive thermal annealings beginning at the 600 K annealing temperature necessary to induce the reaction to form TBP on Cu(100), it was found that a 15 minute annealing at 800 K was necessary in order to observe the formation of molecular structures on the surface that resemble TBP. However, other chemical species were also observed. A few distinct structures are highlighted in Figure 6b.

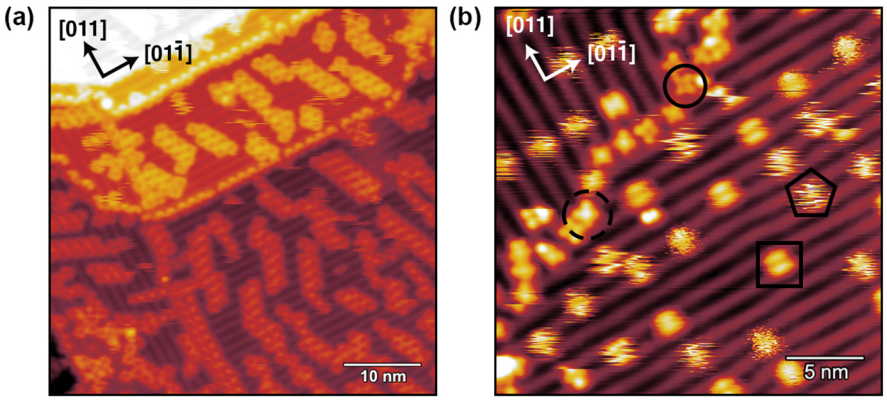

Figure 6. (a) STM image of OEP on Au(100) ($U = -1$ V, $I = 100$ pA) (b) STM image of the products of a 15 minute annealing at 800 K. TBP molecules are observable along a domain boundary of the reconstruction. Distinct species are highlighted with outlined shapes ($U = +1$ V, $I = 100$ pA).

The circled molecule denotes what may be defined as a TBP molecule, where the domain boundary of the Au(100) reconstruction results in molecule–substrate interactions that firmly anchor the molecule to the surface, allowing for clear STM imaging and the identification of the molecular structure. Additionally, along this domain boundary, there is some evidence of metalation of the porphyrin cores by Au atoms. The center of the molecule that otherwise appears as a cavity now appears brighter than the surrounding molecular structure, as marked with a dashed circle in Figure

6b, an effect that is often observed in STM imaging of metalloporphyrins[22] and which has specifically been previously observed for the self-metalation of a porphyrin derivative on Au(111).[33] The STM image presented in Figure 6b also shows the presence of two other distinct species that are marked with a pentagon and square. These species may tentatively be assigned to porphyrin derivatives with constrained rotations that result in their unique appearances. As these species remain stable in their position during STM scanning, the motion apparent in images is rotational in nature, thus resulting in the observed features.[58-59] Overall, the reconstruction of the Au(100) surface appears to constrain molecular diffusion, while the substrate identity results in the need for elevated thermal annealing in order to induce the dehydrocyclization reaction of OEP.

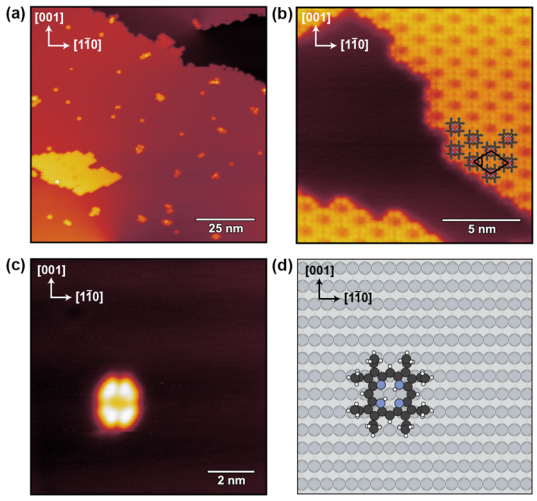

Figure 7. (a) STM image of OEP on Ag(110). Stable self-assembled molecular islands and individual isolated molecules are both evident ($U = +0.1$ V, $I = 2$ nA). (b) Zoomed-in STM image of two molecular islands. All molecules are found to adopt identical orientations on the surface. Molecular models and a unit cell are overlaid. The dimensions of the unit cell are 1.05 nm $\times$ 1.34 nm where the designated angle is 67°. ($U = +1$ V, $I = 150$ pA). (c) STM image of a single OEP molecule on Ag(110) representative of the orientation of all observed molecules on the surface, including for molecules within the self-assembled molecular islands ($U = +0.5$ V, $I = 150$ pA). (d) Illustration of the orientation of a molecular model of OEP on the Ag(110) atomic lattice.

Beyond the substrate identity, the lattice plane of the substrate can have significant effects on self-assembly and surface-catalyzed reactions. To that end, OEP was deposited onto a Ag(110) substrate where the anisotropic surface is expected to result in stronger molecule–substrate interactions due to the atomic scale corrugation that results in a less highly coordinated surface compared to Ag(100).[60-61] Indeed, this effect is immediately apparent following the vapor deposition of OEP onto Ag(110). As shown in Figure 7a, it is possible to observe self-assembled molecular islands, as well as individual isolated molecules that remain stable on the surface independent of the bias voltage applied while scanning, in contrast to the situation observed for OEP on Ag(100). Zooming in on a self-assembled island (Figure 7b) reveals that all of the OEP molecules adopt the same orientation on the surface, as represented with molecular models. Notably, the self-assembly again appears to be mediated by intermolecular interactions between the peripheral alkyl groups as molecules in adjacent rows appear to fit together nicely in a zipperlike manner. However, in this case, since all the OEP molecules adopt identical orientations, a smaller unit cell is observed, perhaps due to the comparatively stronger molecule–substrate interactions found on the Ag(110) surface. As previously mentioned, individual isolated OEP molecules were observed in STM images (Figure 7c). This resulted in the ability to determine the orientation of an OEP molecule relative to the close packed directions of the substrate, as illustrated in Figure 7d. Interestingly, all of the OEP molecules appear to adopt this orientation on the surface, regardless of if they occur in isolation or as part of a molecular island. This suggests a comparatively strong molecule–substrate interaction in contrast to the self-assembled molecular islands of OEP observed on Ag(100).

It was found that a thermal annealing at 700 K was necessary to induce the reaction of OEP molecules on the Ag(110) substrate, resulting in the observation of new chemical species on the

surface. The STM image shown in Figure 8a suggests that these molecules are again TBP, based on their apparent shape. Additionally, all of the molecules adopt the same orientation on this surface, as shown in the aforementioned figure and more clearly with an illustration in Figure 8b. There is also some evidence suggesting metalation of the porphyrin core of some molecules, where the center appears brighter due to the presence of a coordinated metal atom compared to the free base form. This conclusion is supported by the fact that the annealing temperature used here is greater than the temperature previously established to induce self-metalation of phthalocyanine molecules on Ag(110).[28]

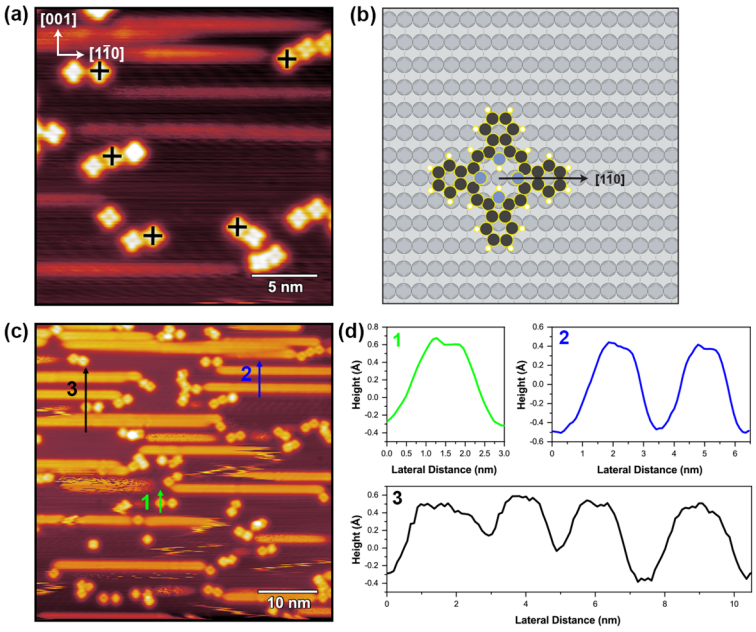

Figure 8. (a) STM image following a 15 minute thermal annealing at 700 K. TBP molecules are observed with molecular models overlaid ($U = -1$ V, $I = 150$ pA). (b) Illustration of the only observed orientation of TBP molecules on Ag(110). The direction of a benzopyrrole subunit is aligned with the $[1\bar{1}0]$ direction. (c) The directions and lengths of extracted line profiles are labeled and color-coded, with the lateral distance and respective tip height plotted adjacent in (d) ($U = +1$ V, $I = 100$ pA). (d) Line profiles extracted from the STM image shown in (b) of a stationary molecule (1) and diffusing species (2) and (3), a dip within in middle of a molecule or diffusing species suggests a porphyrin derivative, where the central cavity appears as a depression in STM imaging.

However, in contrast to other surfaces, diffusing species are clearly evident on the surface as shown in Figure 8c. These species are found to diffuse only along the $[1\bar{1}0]$ direction of the substrate, in line with the atomic rows of the Ag(110) surface which may act as tracks.[62-63] This directional diffusion is independent of the fast and slow scan directions of the STM tip, as shown in the Supporting Information (Figure S3). STM line profiles, extracted from Figure 8c and shown in Figure 8d, across different chemical species provide tentative identification. A line profile across a stable molecule (1) on the surface reveals a dip across the center, characteristic of a free base porphyrin, while the overall molecular structure apparent in STM imaging indicates that these molecules are TBP. Comparing this STM line profile with others across diffusing species (2) and (3) suggests that these molecules that diffuse along the $[1\bar{1}0]$ direction share similar dimensions in STM imaging with the more stable TBP molecules, suggestive of porphyrin derivatives. Overall, the Ag(110) surface was found to result in distinct on-surface molecular behavior compared to the Ag(100) surface, both in terms of the behavior of OEP prior to the reaction (stable self-assembled molecular islands and individual molecules) and following the thermally-induced reaction of OEP to TBP (species were observed diffusing along the $[1\bar{1}0]$ direction).

CONCLUSION

In conclusion, the self-assembly, molecular behavior, and thermally induced reaction of OEP has been investigated on various noble metal surfaces with STM. The substrate identity as well as lattice plane were found to significantly affect the on-surface molecular dynamics, with the ability to influence molecular diffusion and self-assembly through an applied electric field only observed on the Ag(100) substrate. All of the surfaces were found to be capable of inducing the dehydrocyclization reaction of peripheral ethyl groups. This process was confirmed with STM imaging where it was possible to observe OEP molecules prior to the reaction and structures

charactistic of TBP following thermal annealing. Significantly, the temperatures necessary were found to vary significantly and alternative reaction products were observed on certain surfaces which exhibited mobility in terms of rotation, on Au(100), or lateral diffusion, on Ag(110). The STM enabled the identification of individual species and their relative orientations based upon the structures apparent in images, providing the means to develop an understanding of the underlying molecule–substrate interactions. Ultimately, fundamental investigations such as these provide insight into the role of molecule–substrate interactions that are essential to efforts to realize functional nanostructures on surfaces that may require intermolecular interactions and surface-catalyzed chemical reactions.

ASSOCIATED CONTENT

Supporting Information. Description of the method used to determine the annealing temperature for OEP on each substrate. STM image of a higher coverage of OEP molecules on Cu(100) that still lacks self-assembly. Series of STM images showing the growth of a molecular island of OEP on Ag(100) due to varying the bias voltage applied during STM scanning. STM images of the reaction products of OEP on Ag(110) where the fast and slow scan directions have been flipped. Summary table of the behavior of reactant and product molecules on the different substrates.

AUTHOR INFORMATION

Corresponding Author

*E-mail: njiang@uic.edu

Notes

The authors declare no competing financial interest.

ACKNOWLEDGMENTS

We acknowledge support from the National Science Foundation (CHE-1944796).

REFERENCES

1. Tait, S. L., Function Follows Form: Exploring Two-Dimensional Supramolecular Assembly at Surfaces. *ACS Nano* **2008**, *2*, 617-21.
2. Bartels, L., Tailoring Molecular Layers at Metal Surfaces. *Nat. Chem.* **2010**, *2*, 87-95.
3. Li, L.; Mahapatra, S.; Liu, D.; Lu, Z.; Jiang, N., On-Surface Synthesis and Molecular Engineering of Carbon-Based Nanoarchitectures. *ACS Nano* **2021**, *15*, 3578-3585.
4. Barth, J. V., Molecular Architectonic on Metal Surfaces. *Annu. Rev. Phys. Chem.* **2007**, *58*, 375-407.
5. Barth, J. V.; Costantini, G.; Kern, K., Engineering Atomic and Molecular Nanostructures at Surfaces. *Nature* **2005**, *437*, 671-679.
6. Wang, Y., et al., Varying Molecular Interactions by Coverage in Supramolecular Surface Chemistry. *Chem. Commun.* **2012**, *48*, 534-536.
7. Palma, C.-A.; Cecchini, M.; Samorì, P., Predicting Self-Assembly: From Empirism to Determinism. *Chem. Soc. Rev.* **2012**, *41*, 3713-3730.
8. Zhang, Y., et al., A Chiral Molecular Propeller Designed for Unidirectional Rotations on a Surface. *Nat. Commun.* **2019**, *10*, 3742.
9. Niederhausen, J., et al., Subtle Fluorination of Conjugated Molecules Enables Stable Nanoscale Assemblies on Metal Surfaces. *J. Phys. Chem. C* **2018**, *122*, 18902-18911.
10. Wang, Y.; Lingenfelder, M.; Fabris, S.; Fratesi, G.; Ferrando, R.; Classen, T.; Kern, K.; Costantini, G., Programming Hierarchical Supramolecular Nanostructures by Molecular Design. *J. Phys. Chem. C* **2013**, *117*, 3440-3445.
11. Schultz, J. F.; Yang, B.; Jiang, N., On-Surface Formation of Metal–Organic Coordination Networks with C···Ag···C and C=O···Ag Interactions Assisted by Precursor Self-Assembly. *J. Chem. Phys.* **2021**, *154*, 044703.
12. Schultz, J. F.; Yang, B.; Jiang, N., Direct Observation of the Geometric Isomer Selectivity of a Reaction Controlled via Adsorbed Bromine. *Nanoscale* **2020**, *12*, 2726-2731.
13. Otero, R.; Gallego, J. M.; de Parga, A. L. V.; Martín, N.; Miranda, R., Molecular Self-Assembly at Solid Surfaces. *Adv. Mater.* **2011**, *23*, 5148-5176.
14. Peyrot, D.; Silly, F., On-Surface Synthesis of Two-Dimensional Covalent Organic Structures versus Halogen-Bonded Self-Assembly: Competing Formation of Organic Nanoarchitectures. *ACS Nano* **2016**, *10*, 5490-5498.
15. Binnig, G.; Rohrer, H.; Gerber, C.; Weibel, E., Surface Studies by Scanning Tunneling Microscopy. *Phys. Rev. Lett.* **1982**, *49*, 57-61.
16. Ho, W., Single-Molecule Chemistry. *J. Chem. Phys.* **2002**, *117*, 11033-11061.
17. Lackinger, M.; Heckl, W. M., A STM Perspective on Covalent Intermolecular Coupling Reactions on Surfaces. *J. Phys. D: Appl. Phys.* **2011**, *44*, 464011.
18. Schultz, J. F.; Li, S.; Jiang, S.; Jiang, N., Optical Scanning Tunneling Microscopy Based Chemical Imaging and Spectroscopy. *J. Phys.: Condens. Matter* **2020**, *32*, 463001.
19. Grill, L.; Hecht, S., Covalent On-Surface Polymerization. *Nat. Chem.* **2020**, *12*, 115-130.

20. Karmel, H. J.; Chien, T.; Demers-Carpentier, V.; Garramone, J. J.; Hersam, M. C., Self-Assembled Two-Dimensional Heteromolecular Nanoporous Molecular Arrays on Epitaxial Graphene. *J. Phys. Chem. Lett.* **2014**, *5*, 270-274.
21. Guisinger, N. P.; Yoder, N. L.; Elder, S. P.; Hersam, M. C., Subnanometer Imaging of Adsorbate-Induced Electronic Structure Perturbation on Silicon Surfaces. *J. Phys. Chem. C* **2008**, *112*, 2116-2120.
22. Gottfried, J. M., Surface Chemistry of Porphyrins and Phthalocyanines. *Surf. Sci. Rep.* **2015**, *70*, 259-379.
23. Li, L.-L.; Diau, E. W.-G., Porphyrin-Sensitized Solar Cells. *Chem. Soc. Rev.* **2013**, *42*, 291-304.
24. Mahapatra, S.; Ning, Y.; Schultz, J. F.; Li, L.; Zhang, J.-L.; Jiang, N., Angstrom Scale Chemical Analysis of Metal Supported Trans- and Cis-Regioisomers by Ultrahigh Vacuum Tip-Enhanced Raman Mapping. *Nano Lett.* **2019**, *19*, 3267-3272.
25. Mahapatra, S.; Schultz, J. F.; Ning, Y.; Zhang, J.-L.; Jiang, N., Probing Surface Mediated Configurations of Nonplanar Regioisomeric Adsorbates using Ultrahigh Vacuum Tip-Enhanced Raman Spectroscopy. *Nanoscale* **2019**, *11*, 19877-19883.
26. Abuelwafa, A. A.; El-Denglawey, A.; Dongol, M.; El-Nahass, M. M.; Soga, T., Influence of Annealing Temperature on Structural and Optical Properties of Nanocrystalline Platinum Octaethylporphyrin (PtOEP) Thin Films. *Opt. Mater.* **2015**, *49*, 271-278.
27. Marbach, H., Surface-Mediated in Situ Metalation of Porphyrins at the Solid–Vacuum Interface. *Acc. Chem. Res.* **2015**, *48*, 2649-2658.
28. Smykalla, L.; Shukrynau, P.; Zahn, D. R. T.; Hietschold, M., Self-Metalation of Phthalocyanine Molecules with Silver Surface Atoms by Adsorption on Ag(110). *J. Phys. Chem. C* **2015**, *119*, 17228-17234.
29. Li, Y.; Xiao, J.; Shubina, T. E.; Chen, M.; Shi, Z.; Schmid, M.; Steinrück, H.-P.; Gottfried, J. M.; Lin, N., Coordination and Metalation Bifunctionality of Cu with 5,10,15,20-Tetra(4-pyridyl)porphyrin: Toward a Mixed-Valence Two-Dimensional Coordination Network. *J. Am. Chem. Soc.* **2012**, *134*, 6401-6408.
30. Sperl, A.; Kröger, J.; Berndt, R., Controlled Metalation of a Single Adsorbed Phthalocyanine. *Angew. Chem. Int. Ed.* **2011**, *50*, 5294-5297.
31. González-Moreno, R., et al., Following the Metalation Process of Protoporphyrin IX with Metal Substrate Atoms at Room Temperature. *J. Phys. Chem. C* **2011**, *115*, 6849-6854.
32. Yin, C.; Peng, Z.; Liu, D.; Song, H.; Zhu, H.; Chen, Q.; Wu, K., Selective Intramolecular Dehydrocyclization of Co-Porphyrin on Au(111). *Molecules* **2020**, *25*, 3766.
33. Cirera, B.; de la Torre, B.; Moreno, D.; Ondráček, M.; Zbořil, R.; Miranda, R.; Jelínek, P.; Écija, D., On-Surface Synthesis of Gold Porphyrin Derivatives via a Cascade of Chemical Interactions: Planarization, Self-Metalation, and Intermolecular Coupling. *Chem. Mater.* **2019**, *31*, 3248-3256.
34. Williams, C. G.; Wang, M.; Skomski, D.; Tempas, C. D.; Kesmodel, L. L.; Tait, S. L., Dehydrocyclization of Peripheral Alkyl Groups in Porphyrins at Cu(100) and Ag(111) Surfaces. *Surf. Sci.* **2016**, *653*, 130-137.
35. Alkauskas, A.; Ramoino, L.; Schintke, S.; von Arx, M.; Baratoff, A.; Güntherodt, H. J.; Jung, T. A., Energy Level Alignment at Metal−Octaethylporphyrin Interfaces. *J. Phys. Chem. B* **2005**, *109*, 23558-23563.
36. Auwarter, W.; Ecija, D.; Klappenberger, F.; Barth, J. V., Porphyrins at Interfaces. *Nat. Chem.* **2015**, *7*, 105-120.

37. Mura, M.; Silly, F.; Burlakov, V.; Castell, M. R.; Briggs, G. A. D.; Kantorovich, L. N., Formation Mechanism for a Hybrid Supramolecular Network Involving Cooperative Interactions. *Phys. Rev. Lett.* **2012**, *108*, 176103.
38. Lauher, J. W.; Ibers, J. A., Structure of Octaethylporphyrin. Comparison with Other Free Base Porphyrins. *J. Am. Chem. Soc.* **1973**, *95*, 5148-5152.
39. Whiteman, P. J.; Schultz, J. F.; Porach, Z. D.; Chen, H.; Jiang, N., Dual Binding Configurations of Subphthalocyanine on Ag(100) Substrate Characterized by Scanning Tunneling Microscopy, Tip-Enhanced Raman Spectroscopy, and Density Functional Theory. *J. Phys. Chem. C* **2018**, *122*, 5489-5495.
40. Mahapatra, S.; Li, L. F.; Schultz, J. F.; Jiang, N., Methods to Fabricate and Recycle Plasmonic Probes for Ultrahigh Vacuum Scanning Tunneling Microscopy-based Tip-Enhanced Raman Spectroscopy. *J. Raman Spectrosc.* **2021**, *52*, 573-580.
41. Nečas, D.; Klapetek, P., Gwyddion: An Open-Source Software for SPM Data Analysis. *Cent. Eur. J. Phys.* **2012**, *10*, 181-188.
42. Ruban, A.; Hammer, B.; Stoltze, P.; Skriver, H. L.; Nørskov, J. K., Surface Electronic Structure and Reactivity of Transition and Noble Metals. *J. Mol. Catal. A: Chem.* **1997**, *115*, 421-429.
43. Guisinger, N. P.; Mannix, A. J.; Rankin, R. B.; Kiraly, B.; Phillips, J. A.; Darling, S. B.; Fisher, B. L.; Hersam, M. C.; Iski, E. V., Amino Acid Immobilization of Copper Surface Diffusion on Cu(111). *Adv. Mater. Interfaces* **2019**, *6*, 1900021.
44. Schultz, J. F.; Li, L.; Mahapatra, S.; Shaw, C.; Zhang, X.; Jiang, N., Defining Multiple Configurations of Rubrene on a Ag(100) Surface with 5 Å Spatial Resolution via Ultrahigh Vacuum Tip-Enhanced Raman Spectroscopy. *J. Phys. Chem. C* **2020**, *124*, 2420-2426.
45. Chiang, N., et al., Conformational Contrast of Surface-Mediated Molecular Switches Yields Ångstrom-Scale Spatial Resolution in Ultrahigh Vacuum Tip-Enhanced Raman Spectroscopy. *Nano Lett.* **2016**, *16*, 7774-7778.
46. Heinrich, B. W.; Ahmadi, G.; Müller, V. L.; Braun, L.; Pascual, J. I.; Franke, K. J., Change of the Magnetic Coupling of a Metal–Organic Complex with the Substrate by a Stepwise Ligand Reaction. *Nano Lett.* **2013**, *13*, 4840-4843.
47. van Vörden, D.; Wortmann, B.; Schmidt, N.; Lange, M.; Robles, R.; Brendel, L.; Bobisch, C. A.; Möller, R., Following the Steps of a Reaction by Direct Imaging of Many Individual Molecules. *Chem. Commun.* **2016**, *52*, 7711-7714.
48. Yun, B.; Florian, B.; Ina, K.; Martin, S.; Florian, V.; Hans-Peter, S.; Hubertus, M.; Gottfried, J. M., Adsorption of Cobalt (II) Octaethylporphyrin and 2H-Octaethylporphyrin on Ag(111): New Insight into the Surface Coordinative Bond. *New J. Phys.* **2009**, *11*, 125004.
49. Guo, C. S.; Sun, L.; Hermann, K.; Hermanns, C. F.; Bernien, M.; Kuch, W., X-ray Absorption from Large Molecules at Metal Surfaces: Theoretical and Experimental Results for Co-OEP on Ni(100). *J. Chem. Phys.* **2012**, *137*, 194703.
50. Otsuki, J., STM Studies on Porphyrins. *Coord. Chem. Rev.* **2010**, *254*, 2311-2341.
51. Diller, K., et al., Investigating the Molecule-Substrate Interaction of Prototypic Tetrapyrrole Compounds: Adsorption and Self-Metalation of Porphine on Cu(111). *J. Chem. Phys.* **2013**, *138*, 154710.
52. van Vörden, D.; Lange, M.; Schmuck, M.; Schaffert, J.; Cottin, M. C.; Bobisch, C. A.; Möller, R., Communication: Substrate Induced Dehydrogenation: Transformation of Octa-ethyl-porphyrin into Tetra-benzo-porphyrin. *J. Chem. Phys.* **2013**, *138*, 211102.

53. Wiengarten, A., et al., Surface-assisted Dehydrogenative Homocoupling of Porphine Molecules. *J. Am. Chem. Soc.* **2014**, *136*, 9346-9354.
54. Seufert, K.; McBride, F.; Jaekel, S.; Wit, B.; Haq, S.; Steiner, A.; Poli, P.; Persson, M.; Raval, R.; Grill, L., Porphine Homocoupling on Au(111). *J. Phys. Chem. C* **2019**, *123*, 16690-16698.
55. Oncel, N.; Bernasek, S. L., The Effect of Molecule-Molecule and Molecule-Substrate Interaction in the Formation of Pt-Octaethyl Porphyrin Self-Assembled Monolayers. *Appl. Phys. Lett.* **2008**, *92*, 133305.
56. Jiang, N.; Chiang, N.; Madison, L. R.; Pozzi, E. A.; Wasielewski, M. R.; Seideman, T.; Ratner, M. A.; Hersam, M. C.; Schatz, G. C.; Van Duyne, R. P., Nanoscale Chemical Imaging of a Dynamic Molecular Phase Boundary with Ultrahigh Vacuum Tip-Enhanced Raman Spectroscopy. *Nano Lett.* **2016**, *16*, 3898-3904.
57. Jiang, N.; Zhang, Y. Y.; Liu, Q.; Cheng, Z. H.; Deng, Z. T.; Du, S. X.; Gao, H. J.; Beck, M. J.; Pantelides, S. T., Diffusivity Control in Molecule-on-Metal Systems Using Electric Fields. *Nano Lett.* **2010**, *10*, 1184-1188.
58. Tierney, H. L.; Calderon, C. E.; Baber, A. E.; Sykes, E. C. H.; Wang, F., Understanding the Rotational Mechanism of a Single Molecule: STM and DFT Investigations of Dimethyl Sulfide Molecular Rotors on Au(111). *J. Phys. Chem. C* **2010**, *114*, 3152-3155.
59. Buchner, F.; Xiao, J.; Zillner, E.; Chen, M.; Röckert, M.; Ditze, S.; Stark, M.; Steinrück, H. P.; Gottfried, J. M.; Marbach, H., Diffusion, Rotation, and Surface Chemical Bond of Individual 2*H*-Tetraphenylporphyrin Molecules on Cu(111). *J. Phys. Chem. C* **2011**, *115*, 24172-24177.
60. Seidel, C.; Awater, C.; Liu, X. D.; Ellerbrake, R.; Fuchs, H., A Combined STM, LEED and Molecular Modelling Study of PTCDA Grown on Ag(110). *Surf. Sci.* **1997**, *371*, 123-130.
61. Yokoyama, T.; Tomita, Y., Central Metal Dependence of Conformation and Self-Assembly of Porphyrins on Ag(110). *J. Chem. Phys.* **2012**, *137*, 244701.
62. Civita, D.; Kolmer, M.; Simpson, G. J.; Li, A.-P.; Hecht, S.; Grill, L., Control of Long-Distance Motion of Single Molecules on a Surface. *Science* **2020**, *370*, 957-960.
63. Li, J.; Berndt, R.; Schneider, W.-D., Tip-Assisted Diffusion on Ag(110) in Scanning Tunneling Microscopy. *Phys. Rev. Lett.* **1996**, *76*, 1888-1891.

TOC Graphic